Desalination and Water Treatment
www.deswater.com
doi: 10.1080/19443994.2016.1178605

57 (2016) 28460–28473
December

Taylor & Francis
Taylor & Francis Group

The survey of Malathion removal using magnetic graphene oxide nanocomposite as a novel adsorbent: thermodynamics, isotherms, and kinetic study

Roshanak Rezaei Kalantary[a,b], Ali Azari[c], Ali Esrafili[b], Kamyar Yaghmaeian[c], Masoud Moradi[b,*], Kiomars Sharafi[d,c]

[a]*Research Center for Environmental Health Technology (RCEHT), Iran University of Medical Sciences, Tehran, Iran, Tel. +98 9123234586; email: rezaei.r@iums.ac.ir (R.R. Kalantary)*
[b]*Department of Environmental Health Engineering, School of Public Health, Iran University of Medical Sciences, Tehran, Iran, Tel. +989124976672; email: A_esrafily@yahoo.com (A. Esrafili), Tel. +98 9183859910; email: moradi.m@tak.iums.ac.ir (M. Moradi)*
[c]*Environmental Health Engineering, School of Public Health, Tehran University of Medical Sciences, Tehran, Iran, Tel. +98 9124528677; email: aliali2890@yahoo.com (A. Azari), Tel. +98 9123311992; email: k_yaghmaeian@yahoo.com (K. Yaghmaeian), Tel. +98 9183786151; email: Kio.sharafi@gmail.com (K. Sharafi)*
[d]*Research Center for Environmental Determinants of Health, Kermanshah University of Medical Sciences, Kermanshah, Iran*

Received 4 February 2016; Accepted 9 April 2016

ABSTRACT

Malathion is a persistent organophosphorous insecticide, which is widely used in industry, agriculture, and public health. The characterization of Magnetic Graphene Oxide (MGO) was determined by scanning electron microscopy, transmission electron microscopy, X-ray diffraction, Fourier transform infrared spectroscopy, energy dispersive X-ray, vibrating sample magnetometer, and zeta potential. The performance of the adsorbent in removing of malathion was evaluated in different operational conditions including pH, contact time, adsorbent dosage, initial adsorbate concentration, and temperature. The Langmuir and Freundlich isotherms and pseudo-first-order and pseudo-second-order models were applied to describe the adsorption process. The results showed that the maximum adsorption capacity was obtained 43.29 mg g^{-1} and equilibrium data fitted well with the Langmuir isotherm and kinetics of reactions obeyed the pseudo-second-order model. It was also found that the adsorption process was dependent on pH and it was spontaneous and exothermic in terms of thermodynamic studies. Desorption experiments implied that MGO has high stability (very low component leaching) and is probable that can be applied as a novel material for malathion removal from aqueous environments.

Keywords: Malathion; Graphene oxide; Thermodynamic; Isotherms; Kinetic

1. Introduction

Malathion (Diethyl dimethoxythiophosphorylthio succinate) is a non-systemic wide-spectrum, persistent organophosphorous insecticide, which is widely used in industry, agriculture, and public health to control sucking and chewing insects on fruits and vegetables through inhibiting cholinesterase enzyme [1,2]. Entrance of this insecticide into the environment and after being confronted with air, water, and food can

*Corresponding author.

1944-3994/1944-3986 © 2016 Balaban Desalination Publications. All rights reserved.

make serious concerns like vomiting, chest tightness, diarrhea, blurred vision, excessive salivation, watery eyes, dizziness, sweating, headaches, giddiness, loss of consciousness, nervous system, immune system, adrenal glands, liver, carcinogenic, and even death [3–5]. Also, it has toxic effects on environmental ecosystems including birds, fishes, other aquatic invertebrates, and honey bees [6]. Thus, severe pesticide regulations have been compulsory by regulatory organizations in order to prevent the presence of pesticides in runoff and finally in receiving water resources [7].

The World Health Organization (WHO) recommended that the level of a single pesticide in drinking water is 0.1 μg/L [8]. The results of some studies in Iran showed that organophosphorous insecticides, especially malathion, levels exceed the recommended amount by WHO; for example, the concentrations of malathion in water sources of Qazvin, Gorganrood river estuary, and Organophosphorous pesticides in surface water of Iran were 18.83, 88.11, and 503.58 μg/L, respectively [9–11]. Malathion hydrolysis, especially in alkali conditions, can produce some more toxic intermediate compounds in water such as Malaoxon, Malathion alpha and beta monoacid, diethyl fumarate, diethyl thiomalate, O,O-dimethyl phosphorodithioic acid, diethyl thiomalate, and O,O-dimethyl phosphorothionic acid [4]. For example, malaoxon is 61 times more toxic than Malathion [12]. This pesticide is high dissolved in water and hardly removed by solid/liquid separation processes such as coagulation and sand filtration [13]. Several methods are available for removal of pesticides, such as photocatalytic degradation, combined photo-Fenton and biological oxidation, advanced oxidation processes, aerobic degradation, nanofiltration, ozonation, adsorption [14]. It has been demonstrated that all these methods are efficient, but adsorption techniques have been considered as an excellent method for effective removal of different types of pollutants by simple and easy operation, easy application, low costs, high efficiency, and eco-friendly nature [15–17]. Graphene oxide (GO), one of the novel adsorbents, with sheets including one-atom-thick two-dimensional layers of Sp^2-bonded carbon, has some advantages: higher specific surface area (theoretical value 2,630 m^2/g) and proper ability in pollutants removal [18]. In comparison with other carbon nanostructure such as carbon nanotubes, this sorbent has condensed matter physics and through the chemical oxidation modification, abundant oxygen-containing functional groups [19] Nonetheless, its separation in aqueous environment is very difficult, due to its small size. Therefore, magnetization of GO can be a good way to facilitate the separation by magnetic field [20]. Also, magnetite (Fe_3O_4) NPs have been taken into account by researchers because of their high applicability, particularly in remediation of environmental pollutants [21]. Thus, the GO in conjunction with Fe_3O_4 can result in production of a magnetic composite with new functional groups which lead to synergistic or complementary activities between each component. As a result, it has many advantages in environmental pollutant removal [19]. Therefore, the aim of this study was to investigate the removal of malathion using magnetic graphene oxide (MGO) from aqueous solution.

2. Material and methods

2.1. Materials

Graphite powder (150–200 mesh), sodium nitrate ($NaNO_3$), iron(III) chloride hexahydrate ($FeCl{\cdot}6H_2O$), iron(II) chloride tetrahydrate ($FeCl_2{\cdot}4H_2O$), sulfuric acid (H_2SO_4), hydrochloric acid (HCl), potassium permanganate ($KMnO_4$), and hydrogen peroxide (H_2O_2) were purchased from Merck, Germany and used without any purification. Technical grade malathion (95% purity) was obtained from Sigma–Aldrich and used as without further purification. Distilled water was used for making the synthetic samples and pH adjustment was conducted using 0.1 M NaOH and 0.1 M HCl solutions.

2.2. Synthesis of graphene oxide (GO)

The synthesis of GO was carried out using natural graphite powder the modification of Hummers' method [22]. Graphite (1.5 g), $NaNO_3$ (1.5 g), and H_2SO_4 (70 mL) were mixed and stirred in an ice bath. Subsequently, 9 g of $KMnO_4$was added slowly. The reaction mixture was warmed to 40˚C and stirred for 1 h. Water (100 mL) was then added and the temperature was raised to 90˚C for 30 min. Finally, 300 mL of water was added slowly, followed by the slow addition of 10 mL of 30% H_2O_2. The mixture was filtered and washed with 0.1 M HCl and water. The GO precipitate was dispersed in a water/methanol (1:5) mixture and purified with three repeated centrifugation steps at 10,000 rpm for 30 min. The purified sample was dispersed in deionized water and centrifuged at 2,500 rpm to obtain the highly exfoliated GO sheets [23].

2.3. Synthesis of magnetic graphene oxide (MGO) nanocomposites

Initially, 0.9 g of GO dispersion was conducted by ultrasound in 250 mL of DI-water by sonication for

1 h. Then, 0.04 mol of $FeCl_3{\cdot}6H_2O$ and 0.02 mol of $FeCl_2{\cdot}4H_2O$ (molar ratio of Fe^{3+}: Fe^{2+} as 2:1) were dissolved in 25 mL of DI-water solution; the obtained mixture was added gradually to the GO solution at room temperature under a nitrogen flow (40 mL/min) with strong stirring. Next, for preparation of magnetite Fe_3O_4 NP, 28% ammonia solution was added dropwise to make a solution with pH 10, the temperature of the solution rose to 80˚C. After stirred for 5 h, the solution was cooled down to room temperature. The obtained magnetic GO was thoroughly washed with deionized water and collected by magnetic separation, dried at 70˚C under vacuum for 12 h [23].

2.4. Magnetic graphene oxide (MGO) characteristics

The X-ray diffraction (XRD) pattern of MGO chitosan was analyzed (D8 Advance, Bruker, Germany) using graphite monochromatic copper radiation (Cu Ka, $\lambda = 1.54$ Å) at 40 kV, 40 mA, and 25˚C. The morphology was observed with a scanning electron microscopy (SEM) (MIRA3, Tescan, Czech Republic) at 5 keV. To characterize the shape and size of the synthesized MNPs, transmission electron microscopy (TEM) (PHILIPS, EM) was used at 100 keV. Magnetization measurements were carried out using a vibrating sample magnetometer (VSM, 7400, Lakeshore, USA) under applied magnetic field at room temperature. Fourier transform infrared spectrophotometer (FTIR) spectra of the MGO composite were obtained using Tensor 27, Bruker, (Germany) model to confirm the functional groups present in the composite.

2.5. Adsorption study

The adsorption of malathion on the MGO was carried out in a 250-mL Erlenmeyer flasks containing 100 mL of the solution in a batch experiment. The effect of pH, contact time, temperature, adsorbent dose, and adsorbate concentration was studied. Initially, the effect of pH on the adsorption capacity and pH optimum was investigated in the range of 3–11. Then, the adsorption equilibrium was determined at the optimum pH (pH 7) for a time period of 2 h; therefore, the adsorption kinetic parameters were calculated as follow: The certain dosage (2.4 g) of the MGO adsorbent was transferred to 100 mL of the malathion solution, with concentration of 75 mg/L, in a 250-mL flask. After the desired contact time (2–120 min) with 30 min time intervals, the adsorbent was magnetically separated from the solution using a magnet. Then, malathion concentration was analyzed by spectrophotometrically (7400CE CECIL) at $\lambda_{max} = 230$ nm of the adsorbate [24]. Finally, in order to determine the thermodynamic parameters, the effect of temperature on the adsorption capacity was evaluated.

The amount of malathion adsorbed (q_e mg/g) was determined as follows:

$$q_e = \frac{(C_0 - C_e)\ V}{M} \tag{1}$$

where C_0 and C_e are the initial and final concentrations of malathion (mg/L), respectively; V is the volume of the solution (L) and M is the weight of the MGO (g).

3. Results and discussion

3.1. Characterization of the adsorbent

Fig. 1 shows the XRD pattern of the crystalline structures of the GO and MGO. The pattern of GO appearing the unique peak at $2\theta = 9.98^\circ$ belongs to (0 0 1) crystal of the GO. Also, two weakened peaks at $2\theta = 22.06^\circ$ and 42.38° are observed. Compared to the (0 0 1) diffraction peak of the GO, the peaks of the GO were significantly disappeared in XRD pattern of the MGO at $2\theta = 9.98^\circ$; this may be due to three following reasons: (1) the exfoliation of GO layers, (2) graphene sheets less agglomerated in the composite, (3) overcoming of strong Fe_3O_4 signals on weak signals of carbon [23,25,26]. The pattern of the MGO shows that the peaks at $2\theta = 30.2^\circ$, 35.6°, 43.3°, 53.7°, 57.1°, and 62.8° correspond to (2 2 0), (3 3 1), (4 0 0), (4 2 2), (5 1 1), and (4 4 0) are consistent with the standard XRD data for the cubic crystalline structures of Fe_3O_4 [27]. The peaks at $2\theta = 30.2^\circ$, 35.6°, 43.3°, and 57.1° are related to maghemite and magnetite and peaks at $2\theta = 53.7^\circ$ and 62.8° correspond to hematite [28]. The XRD pattern confirmed the presence of Fe_3O_4 particles within the structure of chitosan; thus, the prepared composite could be removed from aqueous solutions by magnetic separation [17].

Figs. 2 and 3 show the infrared spectrum of MGO, GO, malathion (A) and that adsorbed malathion on MGO nanoparticles' surface (B). The wave numbers in the range of 2,960 and 1,450 cm^{-1} represent asymmetrical C–H stretches, while those at 2,940 and 1,375 cm^{-1} attributed to asymmetrical C–H stretches. Two spectra peaks at 1,000–1,200 cm^{-1} and bands at 2,250 cm^{-1} indicate C–O groups and S–H bonds, respectively. The C=O, Methyl and C=C groups stretching vibrations manifested themselves through the peaks at 1,730, 1,380, and 1,640 cm^{-1}, respectively.

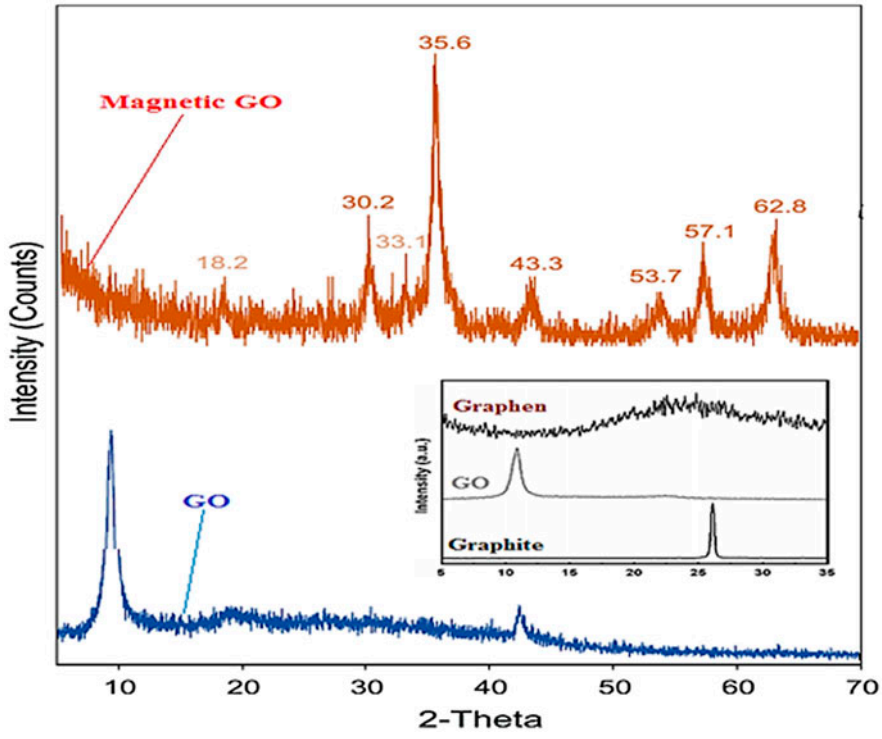

Fig. 1. XRD patterns of GO and MGO.

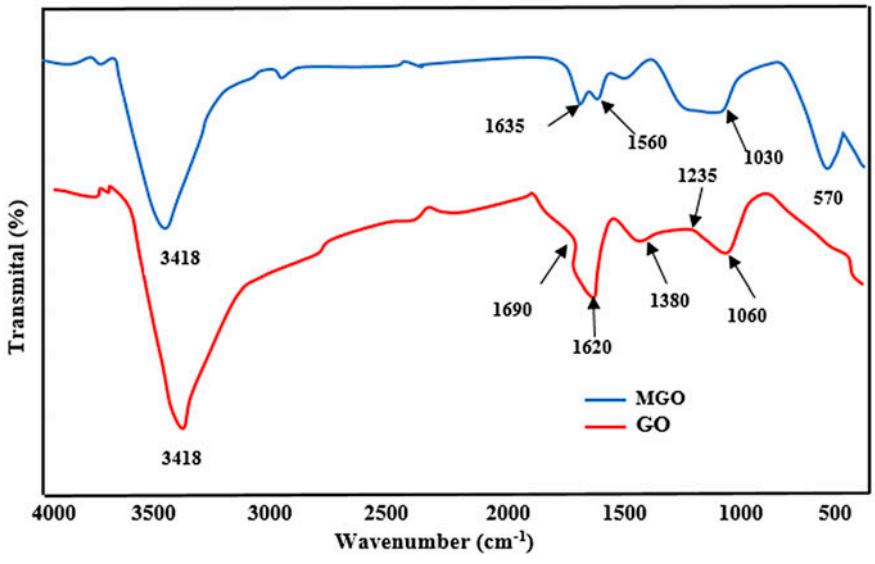

Fig. 2. Infrared spectrum (FT-IR) of MGO and GO.

Other characteristic bonds, appeared at 1,010–1,100 cm^{-1} and also both 655–1,515 cm^{-1} are resulted from P–O bonding, C–C stretch bonds, and P–S bond, respectively [29,30]. After the adsorption process, the peak at about 1,380 cm^{-1} was disappeared, while the two new peaks at 1,548–1,730 were produced, which may be due to P=S and C=O groups of malathion. It was also observed from our energy dispersive X-ray (EDX) results that S and P elements were introduced after the adsorption of the insecticide (Table 1).

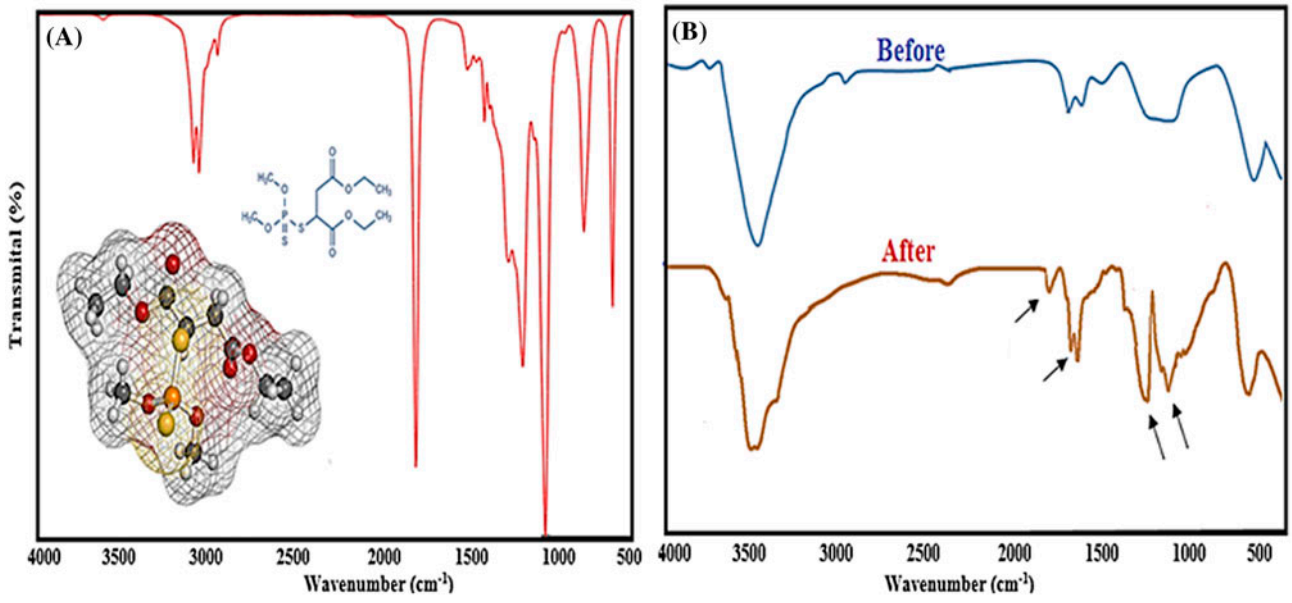

Fig. 3. Infrared spectrum (FT-IR) of malathion (A) and malathion adsorbed on MGO nanoparticles' surface (B).

Additionally, peak at 1,010 cm^{-1} corresponds to the P–O stretching vibration; it is found that the sharp peak becomes a wide peak and the position shifts to 1,234–1,355 cm^{-1} after the adsorption by the MGO. This change can be attributed to the interaction of the MGO with the phosphoric group in the malathion molecules [23,31,32]. The EDX measurement was carried out to further characterize the composition and structure of the MGO composite. As shown in Fig. 4, the EDX analysis of the MGO sample reveals the presence of C, O, and Fe as major elements. On the basis of the aforementioned data, the grafting of Fe_3O_4 onto GO can be concluded.

Fig. 5 shows the SEM image of the GO, Fe_3O_4 and MGO composite at 5 keV. SEM analysis showed that the external adsorbent surface had irregular clumps cavities; this rough and course surface affords proper reactive sites and high adsorption capacity for the adsorbent. This suggests that the GO sheets can act as a worthy support for the embedment of the Fe_3O_4 nanoparticles. Moreover, magnetic Fe_3O_4 particles are closely involved in the surface of graphene, which

Table 1
Elemental composition of MGO after adsorption process

Elements	Atomic weight after adsorption (%)
Carbon	74.14
Oxygen	9.58
Iron	13.11
Sulfur	2.01
Phosphorus	1.16

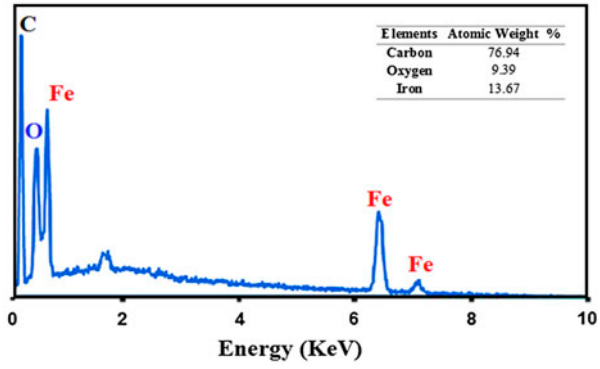

Fig. 4. EDX image of MGO composite.

actually acts as a magnetically inactive layer at the surface of magnetic surface in the composite system, thereby affecting the uniformity or magnitude of magnetization [33].

The morphology of the GO and MGO were characterized by TEM (Fig. 6). Besides, as can be clearly seen from the TEM image, Fe_3O_4 particles with cubic structure have been coated on the GO surface and they have been aggregated because of their exceedingly small size and dipole–dipole coupling. This confirms that the nanosized Fe_3O_4 particles have been successfully synthesized. Herein, the color of the cubic' center is darker, verifying the existence of Fe_3O_4. The many wrinkles on the GO sheets were observed demonstrating an irregular and ribbon-like shape, which conserved a large surface area [18,34].

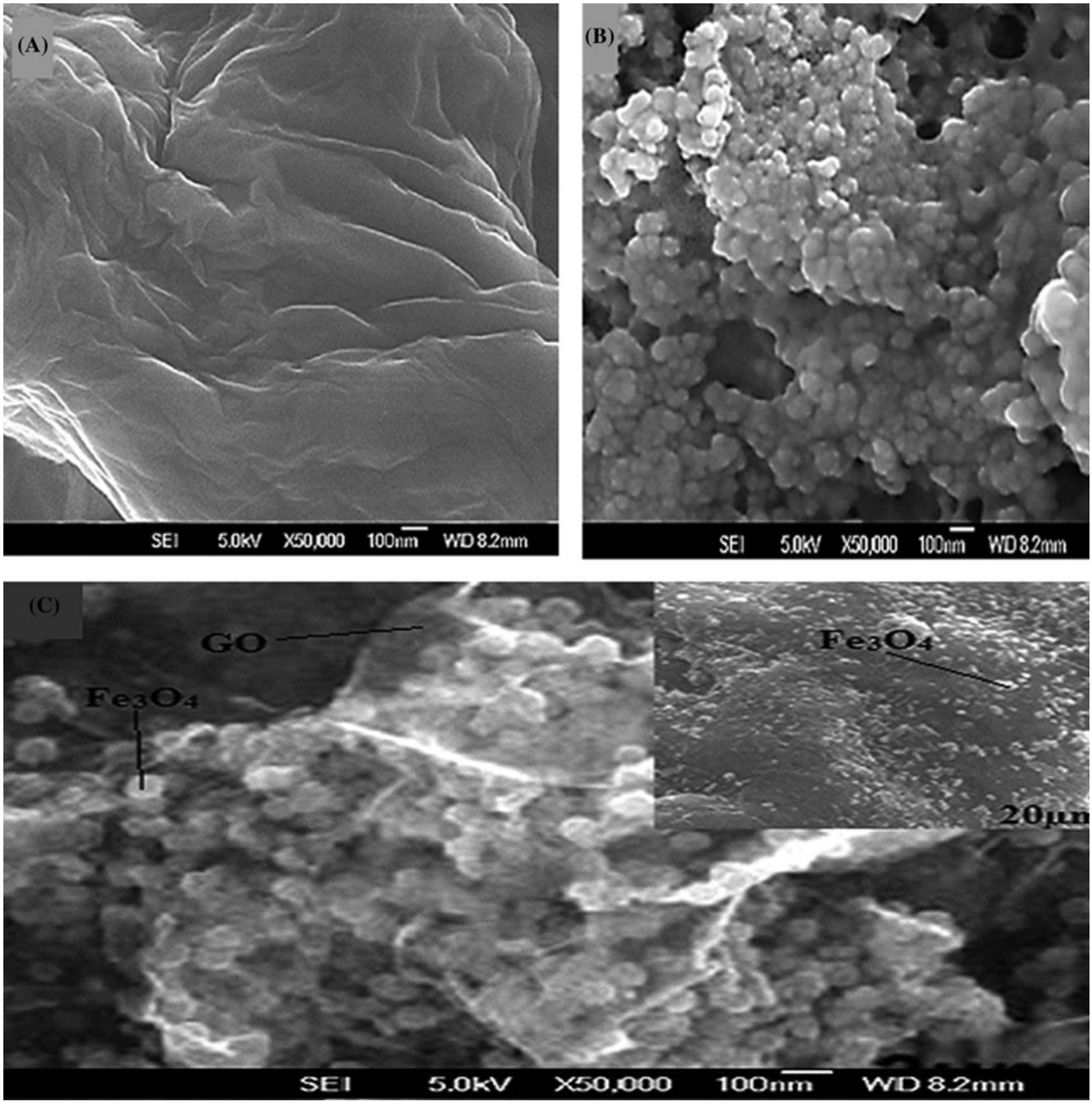

Fig. 5. SEM image of GO (A), Fe_3O_4 (B), and MGO (C).

Fig. 7 shows the magnetization hysteresis loops of the MGO and Fe_3O_4 at room temperature. The results revealed that the magnetization saturation value of MGO and Fe_3O_4 were 38.5–47.2 emu g^{-1}, respectively. As the S curve is indicative of a superparamagnetic characteristic behavior without remanence and coercivity. The magnetization value for the MGO composite was less than that of the naked Fe_3O_4, which can be due to the presence of the non-magnetic GO on the surface of the magnetic particles and nanoscale size of Fe_3O_4 NPs [19,34]. These results ensure that the composite can potentially be applied as a magnetic adsorbent to remove contaminants from aqueous environments, thereby avoiding the generation of secondary pollution [17].

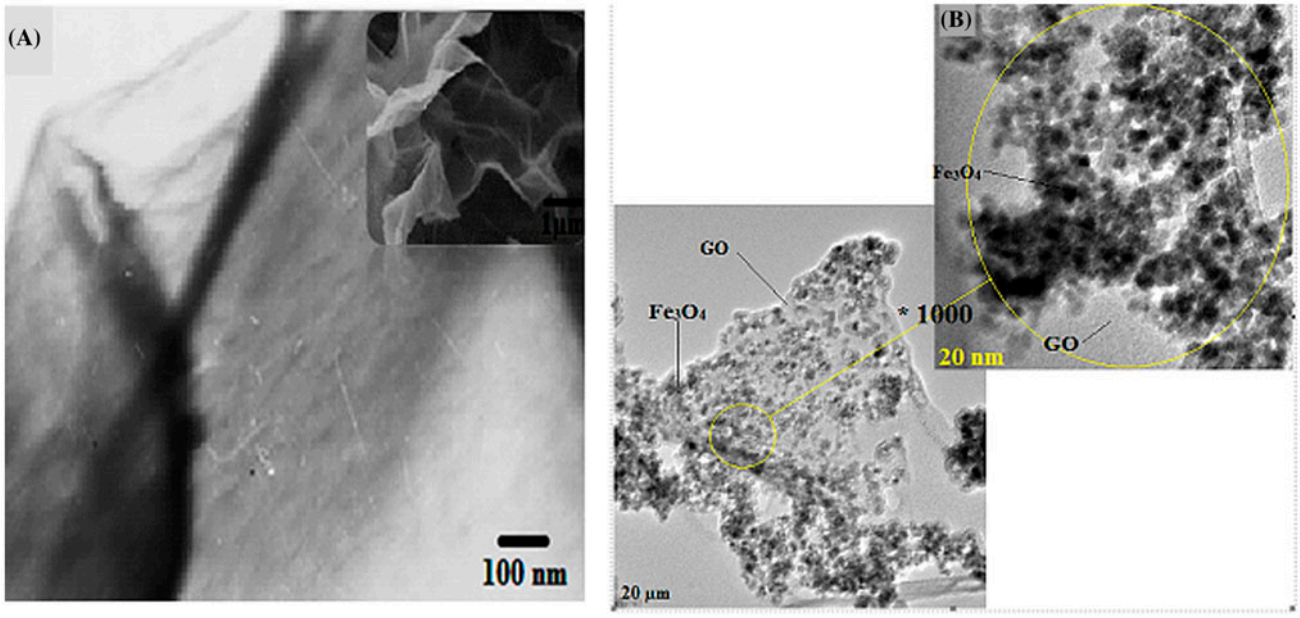

Fig. 6. TEM image of GO (A) and MGO (B).

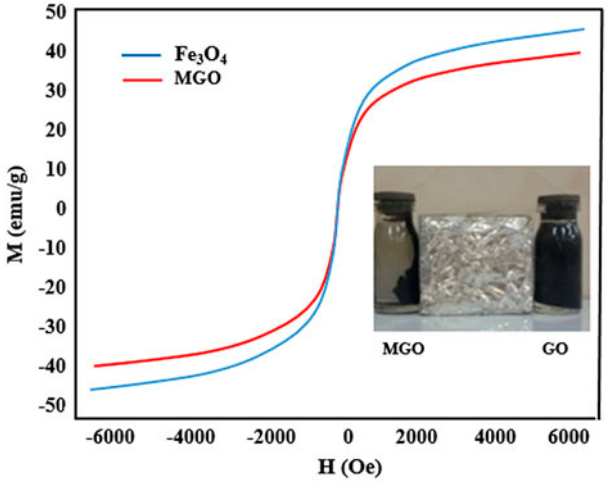

Fig. 7. VSM image of Fe_3O_4 and MGO.

3.2. Effect of initial pH

The main factor in adsorption process is pH solution influencing the surface charge of adsorbents, degree of pollutant ionization, detachment of functional groups on the active sites of adsorbents, as well as physicochemical properties of adsorbate molecule [12,30]. Fig. 8 shows the effect of initial solution pH on removal efficiency of malathion. As can be seen, the efficiency removal of the insecticide is more than alkali condition in acidic condition, so that efficiency removal had an increasing trend at pH 3 (47%) to pH 7 (93%), and, correspondingly, a decreasing trend by increasing pH at alkali conditions. It is a positive point, because the pH of malathion-contaminated aqueous environment normally ranges between 6 and 8. Decreasing malathion adsorption capacity at lower pH values than natural pH values can be due to the protons competition with the malathion molecules for the available adsorption sites [19]. In addition, in acidic conditions, the amount of malathion removal can be due to the presence of plenty of oxygen atoms on the GO in the forms of epoxy, hydroxyl, and carboxyl groups, which are highly agreeable strong electrostatic interactions to positively charged molecules [35]; therefore, at acidic conditions, oxygen atoms may have electrostatic interactions with its di (ethoxycarbonyl) ethyl and dimethyl branches. However, alkali conditions are helpful for the ionization of the oxygen-containing functional groups on the surface of the GO. Moreover, the surface functional groups may become more deprotonated and this makes the frail interaction between the MGO and malathion molecules [12]. Additional reasons for favorable removal of malathion by the MGO can be an attractive interaction of both graphene and pesticide with water molecules and make Graphene-Water-Pesticide (G-W-P) complexes through electrostatic interaction. Therefore, the adsorption of malathion on graphene was possible in the presence of water molecule. Moreover, interaction between GO/Fe_3O_4 surface and π–π Electron

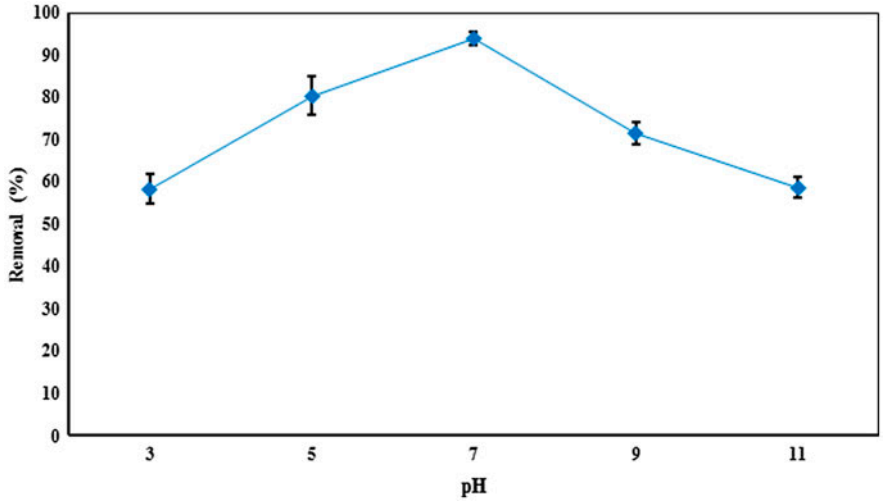

Fig. 8. Effect of solution pH on the adsorption of malathion onto MGO (initial concentration: 75 mg L^{-1}, adsorbent dose: 2.4 g/L, contact time: 45 min, temperature: 30 ± 1).

donor-acceptor of the pollutant is other way for removal of pollutants by GO/Fe_3O_4, which greater polarity of adsorbates leads to higher adsorption capacity [36]. These results were proven by other studies, for instance, the study by Gupta et al. showed optimum pH for the removal of malathion is 6.0 [37]. The study by Senthilkumaar et al. and Sitko et al. indicated that the adsorption was favored in acidic conditions [1,38]. The pH_{zpc} of the MGO was obtained at three. At pH > pH_{ZPC}, the adsorbent surfaces are net negatively charged, which could develop the carboxylate groups in the ranges of pH 3–7; resulting these groups provide further removal of malathion [38,39].

3.3. Adsorption kinetics

The effect of contact time on sorption of malathion onto the MGO adsorbent was studied. The sorption capacity increased severely with increasing contact time; so that just the efficiency removal was reached 70.88–91.92%, respectively, at contact times of 5–20 min. Meanwhile, time necessary to reach the equilibrium was 120 min. It is revealed that enormous vacant active sites may be existence in the adsorbent surface [40], which over time these active sites are occupied by the adsorbate that finally leads to a saturated adsorbent surface [17]. Yang et al. indicated that GO can remove the pollutant more rapidly than other adsorbents by carbon structure [35]. Thus, the adsorption process occurs rapidly as Yao et al. reported that just 30 min was required to reach equilibrium for methylene blue and Congo red adsorbed onto the magnetic Fe_3O_4@graphene nanocomposite, but Jusoh et al. showed that equilibrium time was 150 min for malathion adsorbed onto activated carbon [23,24]. The pseudo-first-order and pseudo-second-order, as two suitable kinetic models, were used in this study for kinetics study of malathion adsorption onto the MGO. The equations of kinetic models are expressed as follows:

$$\text{Pseudo-first-order: } \ln(q_e - q_t) = \ln q_e - k_1 t \quad (2)$$

$$\text{Pseudo-second-order: } t/q_t = t/q_e + 1/K_2 q_e^2 \quad (3)$$

where q_e is the amount of Malathion adsorbed per unit mass of the adsorbent at equilibrium (mg/g), q_t is the amount of malathion adsorbed at time t (mg/g), and k_1 (L min^{-1}) and k_2 (mg g^{-1} min^{-1}) are the coefficients of reaction rate for the pseudo-first-order and the pseudo-second-order models, respectively. Table 2 shows the values of kinetic parameters by linear regression for the two models for malathion adsorption onto the MGO. Considering the correlation coefficients (R^2) and lower deviation between experimental and calculated q_e values, the adsorption of malathion was fitted by the pseudo-second-order model [19]. Essentially, in many cases, the pseudo-first-order model does not fit properly to the whole range of contact time and is usually appropriate over the initial stage of the adsorption processes [19]. Also, the rate-limiting step of the adsorption process was chemical sorption because of the pseudo-second-order kinetic model that accords to the assumption; it could be concluded chemical interaction might be involved in the adsorption process [30].

Table 2
Adsorption kinetic parameters for malathion adsorption onto MGO

Pseudo-first-order					Pseudo-second-order		
C_0	$q_{e,exp}$	K_1 (min^{-1})	$q_{e,cal}$	R^2	K_2 (g mg^{-1} min^{-1})	$q_{e,cal}$	R^2
25	10.41	0.406	4.36	0.8624	0.1717	10.48	0.9999
50	20.83	0.582	1.47	0.9668	0.04	21.09	0.9999
75	30.85	0.66	1.36	0.9052	0.015	31.14	0.9998
100	35.18	0.046	2.49	0.9661	0.0087	36.1	0.9997
125	42.31	0.661	2.23	0.9192	0.0056	43.85	0.9995
150	47.48	0.66	2.41	0.7987	0.00358	49.05	0.9996

The pseudo-second-order rate constant (k) of the pseudo-second-order model was adopted to calculate the activation energy (E_a) of adsorption using the following Arrhenius equation:

$$K = A \exp\left(-\frac{E_a}{RT}\right) \quad (4)$$

where k_2 is the rate constant for pseudo-second-order adsorption kinetics (g/mg min), A is the temperature-independent Arrhenius factor (g/mg min), E_a is the activation energy (kJ/mol), R is the gas constant (8.314 J/mol K), and T is the temperature (K).

The E_a could be obtained from the slope of the line plotting ln k_2 vs. $1/T$ and was 109.57 kJ/mol ($R^2 > 0.99$) at room temperature. The amount of the E_a yields information on the physical or chemical nature of adsorption. Physisorption and chemisorption are usually in the range of $5 < E_a < 40$ kJ/mol and $40 < E_a < 800$ kJ/mol, respectively. The value of the activation energy confirms the nature of the chemisorption of malathion onto the MGO adsorbent [41].

3.4. Effect of adsorbent dose

Fig. 9 shows the variations of the removal efficiency of malathion by the MGO; as figure illustrates, the removal efficiency increased significantly by an increase in the adsorbent dose, from nearly 31.7% at the adsorbent dose of 0.4 g L^{-1} to about 98.66% at the dose of 4.8 g L^{-1}. This can be justified by the fact that the increased adsorbent dose increases the accessibility of active sites on the specific surface area of the MGO, which leads to a boosted removal efficiency of malathion [42]. However, increased adsorbent dose most likely increases particle interactions, such as aggregation and overlapping of active sites, this leads to a significant decrease in the active surface area of the adsorbent and, consequently, decreases its adsorption capacity [17,24].

3.5. Adsorption isotherms

Equilibrium adsorption isotherms describe how an adsorbate interacts with an adsorbent in solution at a certain temperature, affording the most important parameter to assess the adsorption capacity of adsorbents and designing a desired adsorption system [19,30]. The adsorption isotherms of malathion on the MGO was conducted at different initial concentrations. The Langmuir and Freundlich isotherm models were used to analyze the equilibrium adsorption data, which can be expressed as [37]:

$$\text{Langmuir isotherm} = \frac{C_e}{q_e} = \frac{1}{bQ_m} + \frac{C_e}{Q_m} \quad (5)$$

$$\text{Freundlich isotherm} = \log q_e = \log K_f + \frac{1}{n} \log C_e \quad (6)$$

where q_e is the amount of malathion adsorbed at equilibrium (mg g^{-1}), C_e is the equilibrium malathion ion concentration (mg L^{-1}), b is empirical constant that indicate affinity of the binding sites related to the energy of adsorption (L mg^{-1}), q_m is the Langmuir monolayer adsorption capacity (mg g^{-1}), K_f is roughly the adsorption capacity, and $1/n$ is adsorption intensity related to the energy of adsorption effectiveness of MGO. The detailed of the Langmuir and Freundlich constants and the calculated coefficients are shown in Table 3. It was found that the correlation coefficients (R^2) obtained for the Langmuir and Freundlich equations were 0.999 and 0.88, respectively, indicating that the Langmuir isotherm had the best fit with the experimental data. This implies that the process of malathion adsorption onto the MGO follows a monolayer and regular and porous structure. Because the adsorption capacity of malathion was 43.29 mg g^{-1}, this could illustrate the large surface area of the MGO. Moreover, the important feature of the Langmuir isotherm can be expressed in terms of a dimensionless constant separation factor (R_L) given by the following equation:

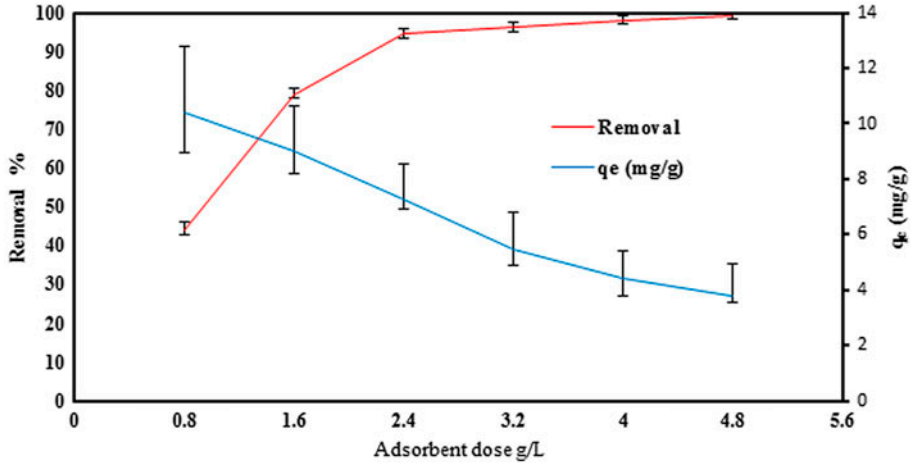

Fig. 9. Effect of adsorbent dose on the removal efficiency and the adsorption capacity of malathion on MGO (pH 7, initial concentration: 75 mg L^{-1}, contact time: 45 min, temperature: 30 ± 1).

$$R_L = \frac{1}{1 + bC_0} \tag{7}$$

where C_0 is the initial concentration in the liquid phase (mg L^{-1}). The value of R_L shows the form of the isotherm to be either unfavorable ($R_L > 1$), linear ($R_L = 1$), favorable ($0 < R_L < 1$), or irreversible ($R_L = 0$) [33], and the R_L values between 0 and 1 indicate favorable adsorption. The R_L value was obtained equal at 0.088 for malathion adsorption onto the MGO. Thus, it approves that the adsorption is a favorable process. As Table 4 shows, the maximum adsorption capacity of the MGO is more than those of other adsorbents.

3.6. Adsorption thermodynamics

The adsorption experiments at different temperatures were conducted to evaluate the influence of temperature on malathion onto MGO in order to provide deeper information on inherent energetic changes, which are associated with adsorption. For this aim, the removal efficiency was calculated at four different temperatures, i.e. 20, 30, 40, and 50°C. Then, the related thermodynamic parameters were calculated by the following equations [17]:

$$\ln K_d = \frac{\Delta S}{R} - \frac{\Delta H}{RT} \tag{8}$$

where ΔS and ΔH are the values of the entropy change (kJ mol^{-1}) and the enthalpy change (J mol^{-1} K^{-1}), respectively, during the process, R (8.314 J mol^{-1} K^{-1}) is the universal gas constant, T (K) is the absolute temperature and K_d is the distribution coefficient, which is be represented as:

$$\ln K_d = \frac{q_e}{C_e} \tag{9}$$

where C_e is the equilibrium concentration of the adsorbate in solution (mg L^{-1}), q_e (mg L^{-1}) is the amount of malathion adsorbed at the equilibrium condition. Meanwhile, the value of the free energy change ΔG can be calculated by:

$$\Delta G = -RT \ln K_d \tag{10}$$

where ΔG is standard free energy (kJ mol^{-1}). Table 5 shows the calculated thermodynamic parameters for the conducted experiments.

The value of ΔG is negative showing the spontaneous nature of the process. Moreover, the absolute values of $-\Delta G$ decreased with increasing temperature;

Table 3
The adsorption isotherm parameters for Malathion adsorption onto MGO

Isotherm model	parameters	
Langmuir	q_m (mg g^{-1})	43.29
	b (L mg^{-1})	0.413
	R_L	0.088
	R^2	0.999
Freundlich	K_f (mg g^{-1})	29.04
	n ($mg^{1-1/n}$ g^{-1} $L^{1/n}$)	3.1
	R^2	0.88

Table 4
Comparison of maximum adsorption capacities for the malathion adsorption onto between various adsorbents found in the literatures

Adsorbent	Optimum pH	Optimum Temp. (°C)	Isotherm	Kinetic	q_{max} (mg g^{-1})	Refs.
Waste" jute fiber carbon	3	30	Langmuir	Pseudo-first-order	37.11	[1]
Rice husk (RH)	6	30	Langmuir	Pseudo-second-order	4.29	[12]
Activated rice husk (ARH)	6	30	Langmuir	Pseudo-second-order	16.13	
Powdered activated carbon (PAC)	6	30	Langmuir	Pseudo-second-order	21.74	
Granular activated carbon (coconut shell)	8.47	60	Langmuir and Freundlich	Not done	909.1	[24]
Granular activated carbon (palm shells)	5.9	60	Langmuir and Freundlich	Not done	555.6	
Bagasse fly ash	6	30	Langmuir and Freundlich	Pseudo-first-order	2.08	[37]
Rhizopus oryzae biomass	6	30	Langmuir and Freundlich	Not done	0.445	[39]
De-acidite FF-IP resin	6	25	Freundlich	Pseudo-second-order	3.5	[42]
Herbal leaves powder (achyranthes aspera)	6	30	Langmuir	Not done	3.401	[43]
Herbal leaves powder (phyllanthus niruri)	6	30	Langmuir	Not done	2.644	
Untreated egg shell	6	25	Langmuir	Pseudo-first-order	1.354	[47]
Thermally treated egg shell at 200°C	6	25	Langmuir	Pseudo-first-order	1.399	
Thermally treated at 400°C	6	25	Langmuir	Pseudo-first-order	1.506	
MGO	7	30	Langmuir	Pseudo-second-order	43.29	This study

this implies that the malathion adsorption on the MGO is not more favorable at higher temperatures [43,44]. Also, the negative value obtained for ΔH shows that Malathion adsorption is an exothermic reaction [37]. Similarly, the value of ΔS was negative, reflecting a decrease in randomness at the solid/solution interface during the adsorption process and there is a strong reaction between the adsorbate and adsorbent [12,45].

3.7. Reusability and stability of MGO

The stability, reuse, and regeneration ability of the adsorbents could be a fundamental key for its applied application and their potential for commercial applications. Components leaching from the adsorbent to aqueous environment may cause secondary contamination. The stability of the MGO composite was evaluated by monitoring the leached Fe content. In this case, the washing of the adsorbent was conducted under acidic, neutral, and basic conditions [46]. As can be seen, the tendency of iron leaching is higher for acidic conditions in comparison with neutral or basic media (Fig. 10). Overall, it can be noticed that the leaching of Fe is practically negligible and was less than the amount of recommended iron for drinking water by WHO (0.3 mg L^{-1}) in the range of pH values between 4 and 10; however, at pH 2–3, the amount of released Fe from the MGO reached over than recommended standards [8].

Because of the Fe stability on MGO surfaces, the composite had high magnetic sensitivity under an external magnetic field. Ai et al. demonstrated that coating by a certain shielding layer was an efficient way to inhibit the Fe leaching from Fe_3O_4; therefore, this subject provides high magnetic sensitivity of

Table 5
Adsorption thermodynamic parameters for malathion adsorption on the MGO

Temp. (K)	ΔG (kJ mol^{-1})	ΔH (kJ mol^{-1})	ΔS (J mol^{-1} K^{-1})
293	−4.36	−18.74	−0.05
303	−4.78		
313	−3.68		
323	−3.08		

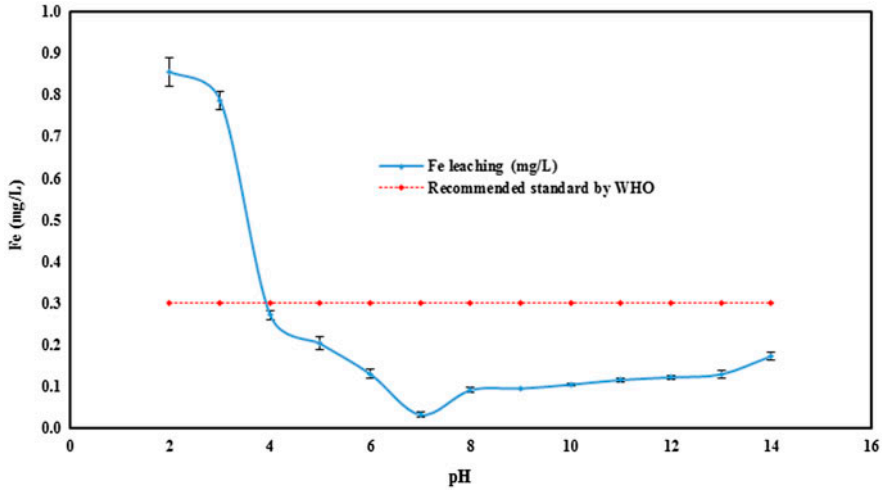

Fig. 10. Tendency of iron leaching under acidic, neutral, and basic conditions.

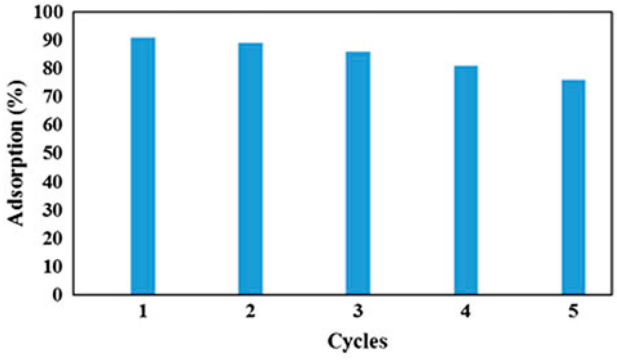

Fig. 11. The malathion adsorption using MGO in five successive cycles of desorption–adsorption.

MGO [19]. The results of several repeated adsorption–desorption cycles have been shown in Fig. 11 illustrating that, after desorption with five cycles, the adsorption capacity of the MGO decreased for each new cycle (92.4 to 85.8%). These findings illustrated that the MGO can potentially be used as a magnetic adsorbent to remove pesticide contaminants from water.

4. Conclusion

Malathion is a persistent organophosphorous insecticide, which is widely used in industry, agriculture, and public health. The combination of GO with Fe_3O_4 in order to produce a magnetic composite would afford an innovative, functional hybrid with synergistic or complementary activities between each component. XRD, SEM, TEM, FTIR, and VSM analyses characterizing the adsorbent revealed a proper adsorbent synthesized. The results indicated that adsorption process was dependent on pH value and the presence of abundant oxygen-containing functional groups (epoxy, hydroxyl, and carboxyl groups) at acidic conditions, can have electrostatic interactions with di (ethoxycarbonyl) ethyl and dimethyl branches of malathion, which provide its further removal in aqueous solution. The maximum adsorption capacity was obtained at 43.29 mg g^{-1} and the Langmuir isotherm had the best fit with the experimental data. Thermodynamic studies indicated that the adsorption process was spontaneous, exothermic and adsorption efficiency increased by a decreased in the temperature. Desorption experiments implied that the MGO had high stability (very low component leaching) and

efficiency removal at least five successive cycles. It is probable that the MGO composite can be applied as a novel material for malathion removal from aqueous environments.

Acknowledgments

The authors wish to warmly acknowledge the invaluable cooperation and support from the Deputy and Chemistry laboratory staff of Iran University of Medical Sciences for facilitating the issue of this project.

References

[1] S. Senthilkumaar, S. Krishna, P. Kalaamani, C. Subburamaan, N.G. Subramaniam, Adsorption of organophosphorous pesticide from aqueous solution using "waste" jute fiber carbon, Mod. Appl. Sci. 4 (2010) 67–83.
[2] N. Venugopal, B. Sumalatha, Spectrophotometric determination of malathion in environmental samples, J. Chem. 9 (2012) 857–862.
[3] K. Mohamed, A. Basfar, H. Al-Kahtani, K. Al-Hamad, Radiolytic degradation of malathion and lindane in aqueous solutions, Radiat. Phys. Chem. 78 (2009) 994–1000.
[4] J.A. Ogunah, C.O. Kowenje, E.T. Osewe, J.O. Lalah, D.A. Jaoko, R.N. Koigi, Effects of zeolites X and Y on the degradation of malathion in water, Science 1 (2013) 7–13.
[5] O. Pal, A. Vanjara, Removal of malathion and butachlor from aqueous solution by clays and organoclays, Sep. Sci. Technol. 24 (2001) 167–172.
[6] M.R. Bonner, J. Coble, A. Blair, L.E.B. Beane Freeman, J.A. Hoppin, D.P. Sandler, M.C. Alavanja, Malathion exposure and the incidence of cancer in the agricultural health study, Am. J. Epidemiol. 166 (2007) 1023–1034.
[7] V.K. Gupta, I. Ali, Removal of endosulfan and methoxychlor from water on carbon slurry, Environ. Sci. Technol. 42 (2008) 766–770.
[8] W.H. Organization, Guidelines for Drinking-Water Quality: Recommendations, World Health Organization, Geneva, 2004.
[9] H. Karyab, A.H. Mahvi, S. Nazmara, A. Bahojb, Determination of water sources contamination to diazinon and malathion and spatial pollution patterns in Qazvin, Iran, Bull. Environ. Contam. Toxicol. 90 (2013) 126–131.
[10] M. Baghfalaki, S.A. Hosseini, R. Ghorbani, A.A. Dehghani, J. Asghari, Monitoring malathion residues in water of the gorganrood riverestuary, Iran, World 5 (2013) 660–663.
[11] A. Fadaei, M.H. Dehghani, S. Nasseri, A.H. Mahvi, N. Rastkari, M. Shayeghi, Organophosphorous pesticides in surface water of Iran, Bull. Environ. Contam. Toxicol. 88 (2012) 867–869.
[12] P. Kumar, H. Singh, M. Kapur, M.K. Mondal, Comparative study of malathion removal from aqueous solution by agricultural and commercial adsorbents, J. Water Process Eng. 3 (2014) 67–73.
[13] K. Ohno, T. Minami, Y. Matsui, Y. Magara, Effects of chlorine on organophosphorus pesticides adsorbed on activated carbon: Desorption and oxon formation, Water Res. 42 (2008) 1753–1759.
[14] M. Vukčević, A. Kalijadis, B. Babić, Z. Laušević, M. Laušević, Influence of different carbon monolith preparation parameters on pesticide adsorption, J. Serb. Chem. Soc. 78 (2013) 1617–1632.
[15] K. Ravikumar, S. Krishnan, S. Ramalingam, K. Balu, Optimization of process variables by the application of response surface methodology for dye removal using a novel adsorbent, Dyes Pigm. 72 (2007) 66–74.
[16] S. Wang, H. Sun, H.-M. Ang, M. Tadé, Adsorptive remediation of environmental pollutants using novel graphene-based nanomaterials, Chem. Eng. J. 226 (2013) 336–347.
[17] A. Mohseni-Bandpi, B. Kakavandi, R.R. Kalantary, A. Azari, A. Keramati, Development of a novel magnetite–chitosan composite for the removal of fluoride from drinking water: Adsorption modeling and optimization, RSC Adv. 5 (2015) 73279–73289.
[18] Q. Han, Z. Wang, J. Xia, S. Chen, X. Zhang, M. Ding, Facile and tunable fabrication of Fe_3O_4/graphene oxide nanocomposites and their application in the magnetic solid-phase extraction of polycyclic aromatic hydrocarbons from environmental water samples, Talanta 101 (2012) 388–395.
[19] L. Ai, Y. Zhou, J. Jiang, Removal of methylene blue from aqueous solution by montmorillonite/$CoFe_2O_4$ composite with magnetic separation performance, Desalination 266 (2011) 72–77.
[20] B. Kakavandi, A.J. Jafari, R.R. Kalantary, S. Nasseri, A. Ameri, A. Esrafily, Synthesis and properties of Fe_3O_4-activated carbon magnetic nanoparticles for removal of aniline from aqueous solution: Equilibrium, kinetic and thermodynamic studies, Iran. J. Environ. Health Sci. Eng. 10 (2013) 10–19.
[21] L. Ai, C. Zhang, Z. Chen, Removal of methylene blue from aqueous solution by a solvothermal-synthesized graphene/magnetite composite, J. Hazard. Mater. 192 (2011) 1515–1524.
[22] D.A. Dikin, S. Stankovich, E.J. Zimney, R.D. Piner, G.H. Dommett, G. Evmenenko, S.T. Nguyen, R.S. Ruoff, Preparation and characterization of graphene oxide paper, Nature 448 (2007) 457–460.
[23] Y. Yao, S. Miao, S. Liu, L.P. Ma, H. Sun, S. Wang, Synthesis, characterization, and adsorption properties of magnetic Fe_3O_4@graphene nanocomposite, Chem. Eng. J. 184 (2012) 326–332.
[24] A. Jusoh, W. Hartini, A. Endut, Study on the removal of pesticide in agricultural run off by granular activated carbon, Bioresour. Technol. 102 (2011) 5312–5318.
[25] J.-H. Deng, X.-R. Zhang, G.-M. Zeng, J.-L. Gong, Q.-Y. Niu, J. Liang, Simultaneous removal of Cd(II) and ionic dyes from aqueous solution using magnetic graphene oxide nanocomposite as an adsorbent, Chem. Eng. J. 226 (2013) 189–200.
[26] M. Moradi, L. Hemati, M. Pirsaheb, K. Sharafi, Removal of hexavalent chromium from aqueous solution by powdered scoria-equilibrium isotherms and kinetic studies, World Appl. Sci. J. 33 (2015) 393–400.

[27] H. Sun, L. Cao, L. Lu, Magnetite/reduced graphene oxide nanocomposites: One step solvothermal synthesis and use as a novel platform for removal of dye pollutants, Nano Res. 4 (2011) 550–562.
[28] M.A. Tofighy, T. Mohammadi, Adsorption of divalent heavy metal ions from water using carbon nanotube sheets, J. Hazard. Mater. 185 (2011) 140–147.
[29] H. Sereshti, S. Samadi, S. Asgari, M. Karimi, Preparation and application of magnetic graphene oxide coated with a modified chitosan pH-sensitive hydrogel: An efficient biocompatible adsorbent for catechin, RSC Adv. 5 (2015) 9396–9404.
[30] Y.-P. Chang, C.-L. Ren, J.-C. Qu, X.-G. Chen, Preparation and characterization of Fe_3O_4/graphene nanocomposite and investigation of its adsorption performance for aniline and *p*-chloroaniline, Appl. Surf. Sci. 261 (2012) 504–509.
[31] K. Urbas, M. Aleksandrzak, M. Jedrzejczak, M. Jedrzejczak, R. Rakoczy, X. Chen, E. Mijowska, Chemical and magnetic functionalization of graphene oxide as a route to enhance its biocompatibility, Nanoscale Res. Lett. 9 (2014) 1–12.
[32] J. Hur, J. Shin, J. Yoo, Y.-S. Seo, Competitive adsorption of metals onto magnetic graphene oxide: Comparison with other carbonaceous adsorbents, Sci. World J. 2015 (2015) 1–11.
[33] H. Wang, X. Yuan, Y. Wu, X. Chen, L. Leng, H. Wang, H. Li, G. Zeng, Facile synthesis of polypyrrole decorated reduced graphene oxide–Fe_3O_4 magnetic composites and its application for the Cr(VI) removal, Chem. Eng. J. 262 (2015) 597–606.
[34] X. Zhu, Z. Mo, C. Zhang, B. Wang, G. Zhao, R. Guo, Preparation of graphene-Fe_3O_4 nanocomposites using Fe^{3+} ion-containing magnetic ionic liquid, Mater. Res. Bull. 59 (2014) 223–226.
[35] S.-T. Yang, S. Chen, Y. Chang, A. Cao, Y. Liu, H. Wang, Removal of methylene blue from aqueous solution by graphene oxide, J. Colloid Interface Sci. 359 (2011) 24–29.
[36] X. Wang, B. Liu, Q. Lu, Q. Qu, Graphene-based materials: Fabrication and application for adsorption in analytical chemistry, J. Chromatogr. A 1362 (2014) 1–15.
[37] V.K. Gupta, C. Jain, I. Ali, S. Chandra, S. Agarwal, Removal of lindane and malathion from wastewater using bagasse fly ash—A sugar industry waste, Water Res. 36 (2002) 2483–2490.
[38] R. Sitko, B. Zawisza, E. Malicka, Graphene as a new sorbent in analytical chemistry, TrAC Trends Anal. Chem. 51 (2013) 33–43.
[39] S. Chatterjee, S.K. Das, R. Chakravarty, A. Chakrabarti, S. Ghosh, A.K. Guha, Interaction of malathion, an organophosphorus pesticide with Rhizopus oryzae biomass, J. Hazard. Mater. 174 (2010) 47–53.
[40] M. Moradi, A.M. Mansouri, N. Azizi, J. Amini, K. Karimi, K. Sharafi, Adsorptive removal of phenol from aqueous solutions by copper (cu)-modified scoria powder: Process modeling and kinetic evaluation, Desalin. Water Treat. 57(25) (2016) 11820–11834.
[41] V.G. Georgieva, M.P. Tavlieva, S.D. Genieva, L.T. Vlaev, Adsorption kinetics of Cr(VI) ions from aqueous solutions onto black rice husk ash, J. Mol. Liq. 208 (2015) 219–226.
[42] M. Naushad, Z. ALOthman, M. Khan, Removal of malathion from aqueous solution using De-Acidite FF-IP resin and determination by UPLC–MS/MS: Equilibrium, kinetics and thermodynamics studies, Talanta 115 (2013) 15–23.
[43] T. Yadamari, K. Yakkala, G. Battala, R.N. Gurijala, Biosorption of malathion from aqueous solutions using herbal leaves powder, Am. J. Anal. Chem. 02 (2011) 37–45.
[44] J. Xu, L. Wang, Y. Zhu, Decontamination of bisphenol a from aqueous solution by graphene adsorption, Langmuir 28 (2012) 8418–8425.
[45] S. Gueu, B. Yao, K. Adouby, G. Ado, Kinetics and thermodynamics study of lead adsorption on to activated carbons from coconut and seed hull of the palm tree, Int. J. Eng. Sci. Technol. 4 (2007) 11–17.
[46] P. Wang, M. Cao, C. Wang, Y. Ao, J. Hou, J. Qian, Kinetics and thermodynamics of adsorption of methylene blue by a magnetic graphene-carbon nanotube composite, Appl. Surf. Sci. 290 (2014) 116–124.
[47] K.Z. Elwakeel, A.M. Yousif, Adsorption of malathion on thermally treated egg shell material, Water Sci. Technol. 61(4) (2010) 1035–1041.